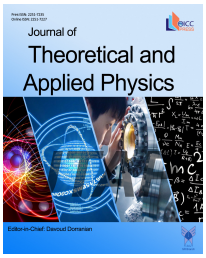

Volume 18, Issue 4, 182453 (1-10)

Journal of Theoretical and Applied Physics (JTAP)

https://dx.doi.org/10.57647/j.jtap.2024.1804.53

Adjusting the operation frequency of cantilever based magnetoelectric sensor

Meisam Haghparast[1], Mohammad Mehdi Tehranchi[1,2,*], Seyedeh Mehri Hamidi[1]

[1]*Laser and Plasma Research Institute, Shahid Beheshti University, Tehran, Iran.*
[2]*Physics Department, Shahid Beheshti University, Tehran, Iran.*

[*]**Corresponding author:** tehranchi@sbu.ac.ir

Original Research

Received:
23 May 2024
Revised:
9 July 2024
Accepted:
24 July 2024
Published online:
30 August 2024

Abstract:

Magnetoelectric sensors, based on magnetostrictive-piezoelectric composites, exhibit the highest sensitivity at electromechanical resonance frequencies. Consequently, adjusting the operation frequency of these sensors for various applications becomes crucial. Using comprehensive simulations based on the finite element method, different structures can be investigated to obtain the operation frequency, magnetoelectric coefficient, and sensitivity. The structures used comprise FeGa/AlN/Silicon sandwich composites in a cantilever-type configuration with the etched silicon substrate. The thickness and etching method of the substrate exert an effect on the mentioned parameters; hence, the operation frequency of these sensors can be adjusted by structural engineering.

Furthermore, this approach enables the identification of optimal structures for applications such as biosensors and energy harvesting. The proposed structure of lower operation frequency exhibits a magnetoelectric coefficient of 3622 V/cm.Oe at a resonance frequency of 965 Hz with a sensitivity of 11.0 pT/$\sqrt{\text{Hz}}$. Subsequently, the superior proposed structure in terms of a magnetoelectric coefficient has 5120 V/cm.Oe at a resonance frequency of 1783 Hz, demonstrating a sensitivity of 3.9 pT/$\sqrt{\text{Hz}}$.

Keywords: Magnetoelectric coefficient; Magnetic field sensor; Finite element method; Magnetostrictive material; Resonance frequency

1. Introduction

Magnetic field sensors with high sensitivity, cost-effectiveness, low power consumption, and small volume are in greatly attend for magnetic field measurement from DC to ultralow frequencies (0 – 100 Hz) [1, 2]. These measurements are needed for various applications, including detecting geomagnetic anomaly fields, exploring geological and mineral resources, intelligent appliances, and biomedical purposes such as magnetocardiography (MCG) and magnetoencephalography (MEG) [3–10]. Using structures with low working frequency for applications such as energy harvesting is also suitable [11, 12].

Currently, there are various methods for detecting weak magnetic fields, including giant magnetoresistance, the Hall effect, atomic magnetometer, superconducting quantum interference device magnetometer (SQUID), anisotropic magnetoresistance, flux-gate meter, magnetoelectric (ME) sensors [13–19]. While SQUID, flux-gate, and atomic magnetometer are highly sensitive, they are highly susceptible to changes in the magnetic flux passing through them. As a result, their sensitivity can be reduced significantly as the sensor dimensions decrease. On the other hand, the ME sensors are more sensitive to the susceptibility distribution around the sensor and thus can be introduced as a high sensitive sensor [20].

ME sensors exploit the magnetoelectric effect, which describes the coupling between the magnetic and electric properties of certain materials. This coupling allows these sensors to transduce between magnetic and electric signals, enabling the detection and measurement of magnetic fields.

At the heart of an ME sensor is a magnetoelectric composite material. These materials are typically made by combining a magnetostrictive phase, which undergoes mechanical deformation in response to an applied magnetic field, and a piezoelectric phase, which generates an electric polarization when mechanically strained. The interaction between these two phases gives rise to the magnetoelectric effect, where an applied magnetic field induces an electric polarization, or vice versa [21, 22].

The performance of the ME sensor is heavily dependent on the properties of the constituent materials. The choice of magnetostrictive and piezoelectric materials can significantly impact the sensor's sensitivity, linearity, and frequency response. Using galfenol alloy with $Fe_{0.83}$ $Ga_{0.17}$ structure due to its high magnetostriction coefficient and AlN with its ability to be used in MEMS provides the required sensitivity and lower electromechanical resonant frequency which works at room temperature. Factors like the composition, microstructure, and interfacial bonding between the magnetostrictive and piezoelectric phases all play a crucial role in optimizing the ME coupling coefficient. Additionally, the geometry and dimensions of the ME composite structure can be tailored to enhance the sensor's performance [19, 23–26].

The ME sensors, which rely on piezoelectric/ferromagnetic composites, have garnered significant attention due to their high sensitivity to magnetic fields, especially at the electromechanical resonance (EMR) frequencies [27, 28]. These sensors hold immense potential for detecting low-frequency magnetic fields, which is crucial for bio-magnetic imaging [29]. Since these sensors are easily integrated, they can be used in micro-electromechanical systems [30].

Recently, various researchers have been trying to reduce EMR frequency and enhance the ME coefficient in the ME sensors. When the frequency of the external AC magnetic field is close to the EMR frequency of the sensor, the maximum ME conversion efficiency can be reached [31, 32].

ME sensors are affected by three crucial factors: piezomagnetism, piezoelectricity, and the coupling between them. To enhance the ME coefficient, appropriate materials must be selected for both phases, and their junctions and coupling mechanisms must be optimized. The elastic coupling between magnetostrictive and piezoelectric materials in composite multiferroics results in the ME effect [33–35]. This effect can be described as the change in electrical polarization of a sample due to a change in magnetization (known as the direct ME effect), or conversely, the change in magnetization due to a change in electrical polarization (known as the inverse ME effect) [36].

However, the resonance frequency of these sensors is usually in the range of several kilohertz, which is higher than the desired low-frequency range. Furthermore, any deviation from the operating frequency can significantly impair the sensor's sensitivity [37–39]. As a result, to measure lower frequency magnetic fields with high accuracy using these sensors, we need to reduce their resonance frequency. Since the sensor's resonance frequency is influenced by its geometry, including parameters like length, area, and mass distribution, we need to explore ways to adjust their operational frequency. Achieving this goal involves designing structures with specific mechanical properties through targeted engineering of the proposed configurations [6, 40, 41]. In this work, by using reliable and accurate simulations based on the finite element method (FEM), we are trying to find a suitable structure for the ME sensor with a high ME coefficient and low operation frequency. By using simulation, it is possible to try different structures and materials while saving time and cost and without laboratory errors, which paves the way for the experimental construction of optimized sensors. We design magnetic field sensors based on Galfenol alloy and Aluminum Nitride (AlN) that cover the cantilever of traditional atomic force microscopes. Additionally, by modifying the geometrical structure of the magnetoelectric composite through silicon substrate etching, we have reduced its operational frequency while striving to maintain a high ME coefficient.

In contrast, for the development of the sensors mentioned above, we use highly sensitive cantilever-type sensors, which exhibit a significant enhancement in the ME coefficient at their EMR frequency. By adjusting the frequency of these cantilever-type sensors, we can shift to specific operational region with the maximum values for both amplitude of the resonance and thus the output voltage of the sensor.

2. Methods and materials

Considering that the ME structures generate electric potential from the applied magnetic field, the ME coefficient (α_{ME}) can be defined as Eq. (1) as a function of E, H, and U as electric field, applied magnetic field, and voltage across the thickness (t) of the piezoelectric layer respectively [42, 43].

$$\alpha_{ME} = \frac{\Delta E}{\Delta H} = \frac{\Delta U}{t.\Delta H} \tag{1}$$

To adjust the operation frequency of the ME sensor, we need to modify the mechanical properties of the structure. For this purpose, we use reliable simulations, using Comsol Multiphysics software based on the FEM technique, to identify the goal structure geometries via proposed chemical etching and obtain the efficiency of them. To model these structures, we need to employ various modules, including Electrostatics, Magnetic Fields, and Solid Mechanics. As illustrated in Figure 1, the ME structures comprise two primary layers: a magnetostrictive layer and a piezoelectric layer. These layers exhibit elastic coupling between them. Our structure utilizes two main layers: Galfenol alloy as the magnetostrictive material and AlN as the piezoelectric material, along with a poly-silicon substrate. For simulation, in addition to the general characteristics of the materials, we defined the piezomagnetic, stiffness, and piezoelectric properties of the material in the software and the main head of the sensor with AC and DC Helmholtz coil placed within an airbox [19].

To achieve maximum sensitivity, the ME sensor is driven to the most sensitive region using a DC bias magnetic field (H_{bias}) that yields the highest value of the ME coefficient. It is an established fact that this region exhibits a linear response with the greatest sensitivity. Here, even small

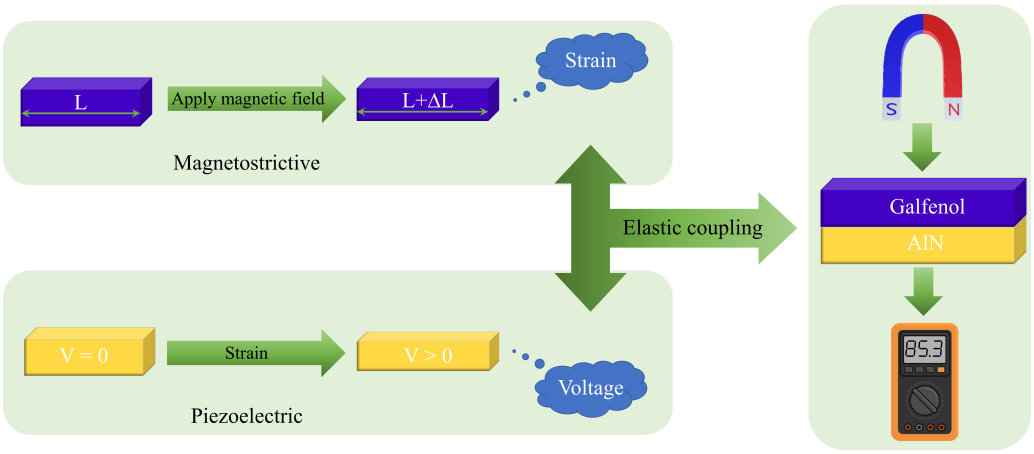

Figure 1. Schematic illustration of ME effect in a composite include magnetostrictive and piezoelectric layers, coupling together with a strain mediation.

variations in the applied magnetic field lead to significant changes in magnetostriction. Considering that the tip's primary frequency depends on the penetration depth of the magnetic field (and thus the structure's thickness), we propose an etching process for the bottom silicon layer in the Galfenol/AlN/Si configuration, defining two distinct categories.

The first category has a magnetostrictive layer with a length and width of 20 mm and 5 mm, respectively. This layer has a thickness of 500 μm. The piezoelectric layer has the exact dimensions as the magnetostrictive layer. The silicon layer used as the substrate has a 20 mm length and 5 mm width, but its thickness varies for different structures. As shown in Figure 2, a part of silicon with a thickness of 200 μm, length of 10 mm, and width of 5 mm was etched. The resulting samples were designated as S_1C_1 through S_6C_1. (Table 1).

The second category of studied structures has the same materials, and the length and width are equal to the first category. But the thickness of both magnetostrictive and piezoelectric layers used in these structures is 250 μm and the main etching region changed to a length and width of 10 mm and 5 mm, respectively, and 150 μm in thickness and the final samples assigned to S_1C_2 to S_6C_2 (Table 1).

3. Results and discussion

Based on the performance of the ME sensors, we need a bias DC magnetic field to reach the maximum sensitivity of these sensors. To calculate this bias magnetic field, we obtain the diagram of magnetization and displacement resulting from applying an external DC magnetic field to the structure for two categories (Figure 3 (a)). As shown in this

Table 1. Etching parameters of the structures according to Figure 2 (b). The green rows are non-etched.

Structure	X (mm)	Y (μm)	X_1 (mm)	X_2 (mm)
S_1C_1	10	200	0	10
S_2C_1	10	200	2.5	7.5
S_3C_1	10	200	5	5
S_4C_1	10	200	7.5	2.5
S_5C_1	10	200	10	0
S_6C_1	0	0	10	10
S_1C_2	10	150	0	10
S_2C_2	10	150	2.5	7.5
S_3C_2	10	150	5	5
S_4C_2	10	150	7.5	2.5
S_5C_2	10	150	10	0
S_6C_2	0	0	10	10

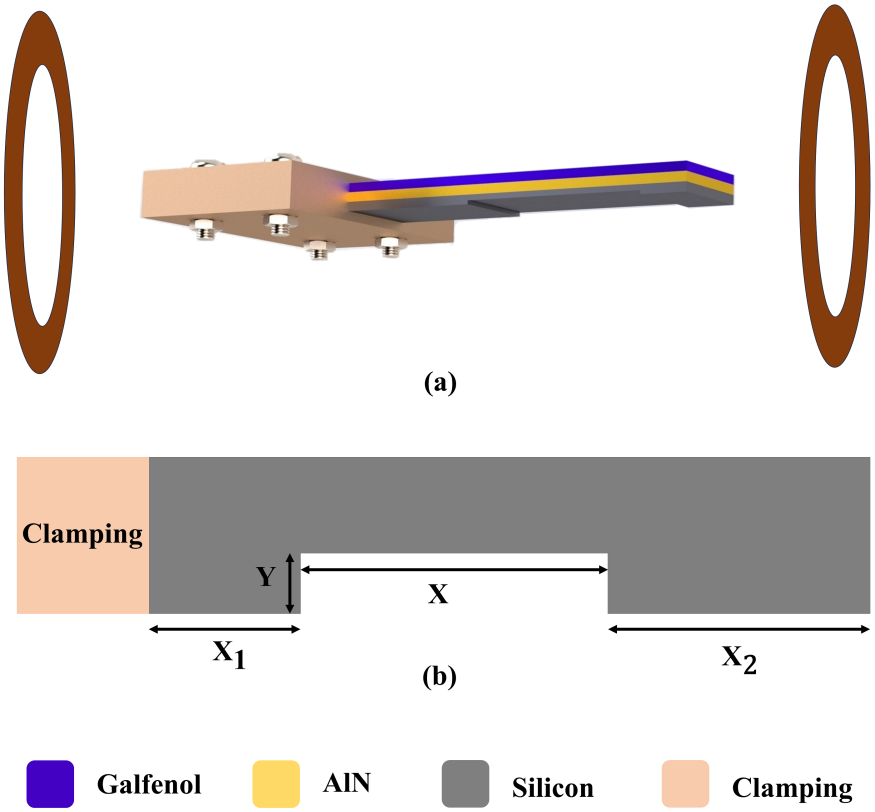

Figure 2. (a) Schematic of the ME structure and Helmholtz coil. (b) Side view of silicon and its etching parameters.

figure, the sensors of the first category with a layer thickness of 500 μm, sweep the bending from 19.9 (S_6C_1) to 25.2 μm (S_1C_1) in the magnetization saturation region. In this category, considering that no etching has been done for the S_6C_1 structure, the ratio of the volume of the magnetostrictive layer to the total volume of the structure is the minimum, and more anchoring between the layers is an obstacle to increasing the amount of bending of the sensor, so it has the slightest bending. The second-category sensors with a thickness of 250 μm show a bending between 39.8 (S_6C_2) and 55.5 μm (S_1C_2), when they are in the magnetization saturation range. Due to the lower thickness of this category, they show less resistance to the external magnetic field, and more bending is created in them than in the first category. In this category, as in the C_1 group, the first sample, which has etching in the clamping part and has a higher weight percentage in the free part, experiences the most bending. By decreasing the weight percentage in the free area and increasing it in the clamped part, the sensor's tail bending decreases as expected. Additionally, the non-etched structure exhibits less bending, approximately 39.8 μm, due to the reduction in the magnetostrictive layer's volume relative to the total volume. The sensor's tail bending values for all samples are mentioned in Table 2.

However, if the thickness of the piezoelectric layer is the same for both categories, more bending causes more voltage in the desired area, and we can rely on these structures to make the sensor. But by changing the thickness of the piezoelectric layer in the second category compared to the first category, the received voltage and the sensitivity of the sensors to the external magnetic field are studied. Therefore, the achievable output voltage from the sensor was calculated for different external magnetic fields until the magnetostrictive layer reached saturation magnetization (Figure 3 (b)). The maximum electric potential of 85.3 and 45.6 volts was obtained for S_1C_1 and S_1C_2 for two categories, respectively. Both of these structures have etched on the clamped side. According to this diagram, for the structures with the same volume ratio of the layers (etched structures), As the etching moves towards the free and oscillating point of the sensor, the voltage received from the sensor decreases (Table 2).

From an application perspective, samples that exhibit higher voltage values when subjected to a magnetic field can be utilized for energy harvesting. Conversely, for sensor application, we need the sensitivity in the magnetic bias area of the structures. For this purpose, we calculate the derivative of the voltage received from the sensor to the applied magnetic field (Figure 3 (c)). According to the data presented in this figure, the structures in the first and second categories exhibit their highest sensitivity at DC magnetic fields of 2.3 mT (1.8 kA/m) and 1.5 mT (1.2 kA/m), respectively. These magnetic fields serve as the bias DC magnetic field for the two categories of structures. The lower bias magnetic field observed in the second category is attributed to the thinner structure dimensions. Consequently, the magnetostrictive phase's magnetic domains rotate more rapidly, positioning them at their most sensitive point.

Considering that the ME coefficient is frequency-dependent, there is a significant disparity between the ME response in the EMR frequency regime and the off-resonance fre-

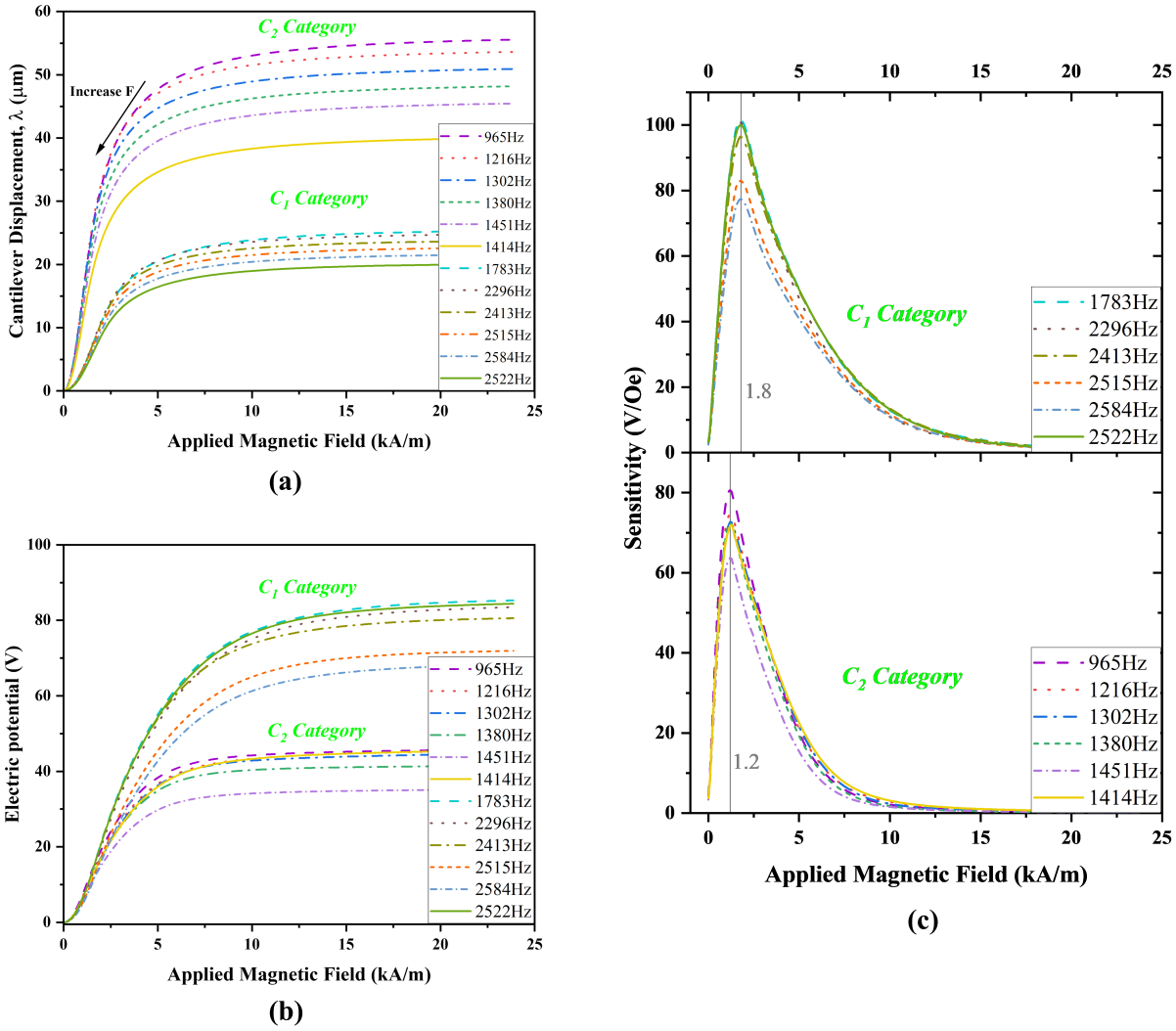

Figure 3. (a) Displacement of the free part of the structures in two categories relative to changes in the applied magnetic field, (b) The maximum achievable output voltage in the structures, (c) The ME structures sensitivity to the applied magnetic field. The modified names in the guide column are the resonance frequency of the structures.

quency range. Using of Comsol Multiphysics software and an Eigenfrequency study, we were able to determine the bending resonance frequency, also known as the first-order resonance frequency, for various structures. The resonance frequency depends on factors such as the material, mass, and geometrical shape of the structure. Using the dynamic method, we accurately determined the EMR frequency and mitigated bending effects resulting from the applied DC magnetic field. The ME effect was simulated using this approach, where a bias DC magnetic field was applied via a Helmholtz coil, while the AC magnetic field was swept by another Helmholtz coil at varying frequencies. The EMR frequency for all structures is presented in Table 2. According to this table, silicon etching on the clamped side and increasing the relative weight in the oscillating part reduces the resonance frequency. The resonance frequencies of structures S_6C_1 and S_6C_2 differ from those of the others, primarily due to the absence of etching and the altered masses of the silicon substrate.

Through FEM analysis and applying 1 Oe.AC magnetic field alongside a bias DC magnetic field, the value of the ME coefficient of the magnetoelectric sensors obtains in terms of volts per meter (Figure 4 (a) and (b)). The samples of the second category reach their maximum value at lower frequencies like S_1C_2 with the ME coefficient of 3622 (V/cm.Oe) at 965 Hz.

However, we can see some equivalent the ME coefficients in two categories like as S_5C_1 and S_1C_2, with ME coefficients 3713 and 3622 V/cm.Oe respectively, the effect of the etching position from the clamped point onto free point of the cantilever is dominate in the selection of the samples for our main aim. This phenomenon arises from the relative weight of the layers at the free point of the structure, which can influence fluctuations when a magnetic field is applied, impacting their overall performance. As a result, we can select the final structure depending on the customer's ordering in sensor or energy harvesting applications from different categories based on our lab's coating equipment.

In experimental work, the lock-in amplifier technique can measure the magnetic field resolution. The experimental

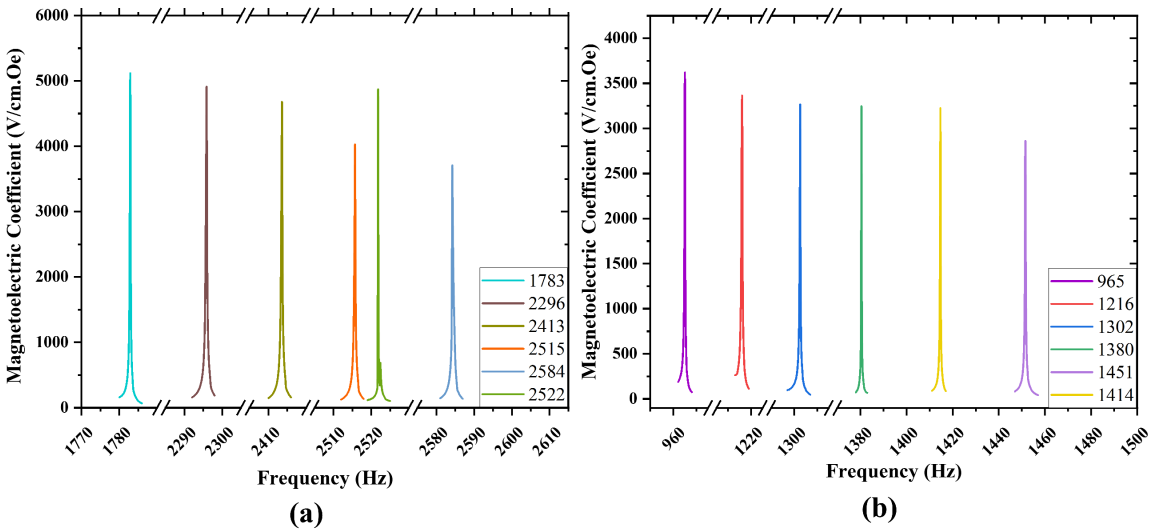

Figure 4. The ME coefficient in EMR frequency for: (a) first category, (b) second category. The modified names in the guide column are the resonance frequency of the structures in Hz.

voltage resolution of the lock-in amplifier is about 10 μV when measuring the electric potential of the piezoelectric layer. Using Eq. (2), the magnetic field resolution for the simulated ME structures is listed in Table 2.

$$S = \frac{E}{\alpha_{\mathrm{ME}}.L} \tag{2}$$

where S is the sensitivity of the ME sensor, E is noise voltage density, α_{ME} is the ME coefficient, and L is the thickness of the piezoelectric layer [44, 45].

As shown in the Table 2, optimizing the structure through engineering and etching, along with frequency adjustments, enhances the sensitivity of the ME composites. Notably, within each category, the S_1 samples with the same etching type exhibit the highest sensitivity. According to the values obtained in this table, these structures can be used as AC magnetic field sensors in the lower frequency range.

Due to the etching performed on the silicon substrate, the increase in the mass ratio in the oscillating part of the cantilever reduces the structure's resonance frequency. On the other hand, reducing the thickness of the magnetostrictive and piezoelectric layers changes the bias magnetic field. This reduction in thickness creates a lower electric potential against changes in the magnetic field and reduces the sensitivity of the C_2 group.

For a better understanding of the simulations, it can be compared with the experimental work done in this field. This comparison provides a clearer perspective on the outcomes we have obtained. Yang Qiu et al. reported that

Table 2. Simulation results for all investigated structures. The green rows are non-etched.

Sample	EMR frequency (Hz)	Cantilever displacement (μm)	Electric potential (V)	α_{ME} (V/cm.Oe)	Sensitivity (pT/$\sqrt{\mathrm{Hz}}$)
S_1C_1	1783	25.2	85.3	5120	3.9
S_2C_1	2296	24.7	83.5	4918	4.1
S_3C_1	2413	23.6	80.5	4679	4.3
S_4C_1	2515	22.5	71.9	4131	4.8
S_5C_1	2584	21.5	67.8	3713	5.4
S_6C_1	2522	19.9	84.4	4865	4.1
S_1C_2	965	55.5	45.6	3622	11.0
S_2C_2	1216	53.6	45.2	3368	11.9
S_3C_2	1302	50.9	44.4	3269	12.2
S_4C_2	1380	48.1	41.3	3246	12.3
S_5C_2	1451	45.5	35.0	2864	13.9
S_6C_2	1414	39.8	45.3	3226	12.4

Metglas/PVDF/Metglas laminates have sensitivity of 36 pT/$\sqrt{\text{Hz}}$ at resonance frequency of 30 kHz [46]. Jingen Wu et al. prepared a self-biased magnetoelectric sensor with a ME coefficient of 48.8 V/cm.Oe at resonance frequency of 107.5 kHz and capacity of detect ac magnetic fields of 4.58 nT at 1 kHz and 10.43 pT at resonant frequency [47]. Fan Li et al. reported that Galfenol/PZT/Galfenol magnetoelectric sandwich devices have a ME coefficient of 55 V/cm.Oe, which is suitable for energy harvesting [48].

4. Conclusion

In summary, the various structures resulting from silicon layer etching allow us to adjust the magnetoelectric (ME) structure for specific applications. The structures S_1C_1, S_2C_1, and S_6C_1 are suitable for use as energy harvesters due to their high electric potential value. S_1C_2 can be used for sensors with low operation frequency so that its resonance frequency is below 1 kHz and has a magnetic field resolution of 11 pT/$\sqrt{\text{Hz}}$. S_1C_1 can be used in applications where sensitivity is essential, the sensitivity of this structure is below 4 pT/$\sqrt{\text{Hz}}$. This can be useful for bio-magnetic sensors to detect small forces generated by biological molecules or magnetic particles. All of these simulations were conducted in both passive and active modes. These results were compared with experimental data, either to validate the simulation outcomes or to mitigate environmental noise. These findings collectively underscore the potential of tailoring composite structures to achieve precise operational parameters, thereby opening vistas for innovative applications in diverse technological domains.

Authors Contributions
All the authors have participated sufficiently in the intellectual content, conception and design of this work or the analysis and interpretation of the data (when applicable), as well as the writing of the manuscript.

Availability of Data and Materials
The data that support the findings of this study are available from the corresponding author upon reasonable request.

Conflict of Interests
The authors declare that they have no known competing financial interests or personal relationships that could have appeared to influence the work reported in this paper.

References

[1] J. Li, G. Ma, S. Zhang, C. Wang, Z. Jin, W. Zong, G. Zhao, X. Wang, J. Xu, D. Cao, and S. Li. "AC/DC dual-mode magnetoelectric sensor with high magnetic field resolution and broad operating bandwidth.". *AIP Advances*, **11**:045015, 2021. DOI: https://doi.org/10.1063/5.0048167.

[2] M. Bichurin, R. Petrov, O. Sokolov, V. Leontiev, V. Kuts, D. Kiselev, and Y. Wang. "Magnetoelectric magnetic field sensors: A review. ". *Sensors*, **21**, 2021. DOI: https://doi.org/10.3390/s21186232.

[3] A. Kumar and D. Kaur. "Magnetoelectric heterostructures for next-generation MEMS magnetic field sensing applications.". *Journal of Alloys and Compounds*, **897**:163091, 2022. DOI: https://doi.org/10.1016/j.jallcom.2021.163091.

[4] Elhussein M Essa KS. "Interpretation of magnetic data through particle swarm optimization: Mineral exploration cases studies.". *Natural Resources Research*, **29**: 521–37, 2020. DOI: https://doi.org/10.1007/s11053-020-09617-3.

[5] Lee H Chun J Maurya D Hwang GT Ryu J Priya S. Kang MG, Sriramdas R. "High power magnetic field energy harvesting through amplified magneto-mechanical vibration. ". *Advanced Energy Materials*, **8**:1703313, 2018. DOI: https://doi.org/10.1002/aenm.201703313.

[6] A. V. Turutin, I. V. Kubasov, A. M. Kislyuk, V. V. Kuts, M. D. Malinkovich, Y. N. Parkhomenko, and N. A. Sobolev. "Ultra-sensitive magnetoelectric sensors of magnetic fields for biomedical applications. ". *Nanobiotechnology Reports*, **17**:261–89, 2022. DOI: https://doi.org/10.1134/s2635167622030223.

[7] M. Ranjbaran, M. M. Tehranchi, S. M. Hamidi, and S. M. H. Khalkhali. "Harmonic detection of magnetic resonance for sensitivity improvement of optical atomic magnetometers. ". *Journal of Magnetism and Magnetic Materials*, **424**:284–90, 2017. DOI: https://doi.org/10.1016/j.jmmm.2016.10.058.

[8] R. Jahns, H. Greve, E. Woltermann, E. Quandt, and R. Knöchel. "Sensitivity enhancement of magnetoelectric sensors through frequency-conversion.". *Sensors and Actuators A: Physical*, **183**:16–21, 2012. DOI: https://doi.org/10.1016/j.sna.2012.05.049.

[9] R.-M. Friedrich, S. Zabel, A. Galka, N. Lukat, J.-M. Wagner, C. Kirchhof, E. Quandt, J. Mccord, U. C. Selhuber, M. Siniatchkin, and F. Faupel. "Magnetic particle mapping using magnetoelectric sensors as an imaging modality. ". *Scientific Reports*, **9**:2086, 2019. DOI: https://doi.org/10.1038/s41598-018-38451-0.

[10] I. Bok, I. Haber, X. Qu, and A. Hai. "In silico assessment of electrophysiological neuronal recordings mediated by magnetoelectric nanoparticles. ". *Scientific Reports*, **12**:8386, 2022. DOI: https://doi.org/10.1038/s41598-022-12303-4.

[11] H. Jafari, A. Ghodsi, S. Azizi, and M. R. Ghazavi. "Energy harvesting based on magnetostriction, for low frequency excitations.". *Energy*, **124**:1–8, 2017. DOI: https://doi.org/10.1016/j.energy.2017.02.014.

[12] N. Jackson, O. Z. Olszewski, C. O'Murchu, and A. Mathewson. "Ultralow-frequency PiezoMEMS energy harvester using thin-film silicon and parylene substrates. ". *Journal of Micro/Nanolithography, MEMS, and MOEMS*, **17**:015005–015005, 2018. DOI: https://doi.org/10.1117/1.JMM.17.1.015005.

[13] D. Murzin, D. J. Mapps, K. Levada, V. Belyaev, A. Omelyanchik, L. Panina, and V. Rodionova. "Ultrasensitive magnetic field sensors for biomedical applications. ". *Sensors*, **20**, 2020. DOI: https://doi.org/10.3390/s20061569.

[14] A. Roy, P. Sampathkumar, and P. S. Anil Kumar. "Development of a very high sensitivity magnetic field sensor based on planar Hall effect.". *Measurement*, **156**:107590, 2020. DOI: https://doi.org/10.1016/j.measurement.2020.107590.

[15] Yin Y Wang Y Zhou B Han B. Liu G, Tang J. "Single-beam atomic magnetometer based on the transverse magnetic-modulation or DC-offset.". *IEEE Sensors Journal*, **20**:5827–33, 2020. DOI: https://doi.org/10.1109/JSEN.2020.2973201.

[16] S. Wissberg, M. Ronen, Z. Oren, D. Gerber, and B. Kalisky. "Sensitive readout for microfluidic high-throughput applications using scanning SQUID microscopy.". *Scientific Reports*, **10**:1573, 2020. DOI: https://doi.org/10.1038/s41598-020-58307-w.

[17] E. S. Oliveros Mata, G. S. Cañón Bermúdez, M. Ha, T. Kosub, Y. Zabila, J. Fassbender, and D. Makarov. "Printable anisotropic magnetoresistance sensors for highly compliant electronics. ". *Applied Physics A*, **127**:280, 2021. DOI: https://doi.org/10.1007/s00339-021-04411-1.

[18] P. M. Vetoshko, N. A. Gusev, D. A. Chepurnova, E. V. Samoilova, I. I. Syvorotka, I. M. Syvorotka, et al. "Flux-gate magnetic field sensor based on yttrium iron garnet films for magnetocardiography investigations. ". *Technical Physics Letters*, **42**:860–4, 2016. DOI: https://doi.org/10.1134/S1063785016080289.

[19] M. Haghparast, M. M. Tehranchi, and S. M. Hamidi. "Magneto electric sensor based on cantilever coated galfenol/AlN structure. ". *Journal of Magnetism and Magnetic Materials*, **572**:170602, 2023. DOI: https://doi.org/10.1016/j.jmmm.2023.170602.

[20] J. Li, K. Sun, Z. Jin, Y. Li, A. Zhou, Y. Huang, S. Yang, C. Wang, J. Xu, G. Zhao, X. Wang, D. Cao, W. Zong, and S. Li. "A working-point perturbation method for the magnetoelectric sensor to measure DC to ultralow-frequency-AC weak magnetic fields simultaneously.". *AIP Advances*, **11**:065213, 2021. DOI: https://doi.org/10.1063/5.0047490.

[21] G. Channagoudra and V. Dayal. "Magnetoelectric coupling in ferromagnetic/ferroelectric heterostructures: A survey and perspective. ". *Journal of Alloys and Compounds*, **928**:167181, 2022. DOI: https://doi.org/10.1016/j.jallcom.2022.167181.

[22] C. Chen, S. Zhong, G. Sun, Y. Zhang, Y. Ding, K. Ren, H. Li, R. Gao, X. Deng, W. Cai, and Z. Wang. "The magnetoelectric coupling effect of multiferroic fluids and their potential applications. ". *Journal of Materials Science: Materials in Electronics*, **34**:2041, 2023. DOI: https://doi.org/10.1007/s10854-023-11490-8.

[23] T. Deng, Z. Chen, W. Di, R. Chen, Y. Wang, L. Lu, H. Luo, T. Han, J. Jiao, and B. Fang. "Significant improving magnetoelectric sensors performance based on optimized magnetoelectric composites via heat treatment. ". *Smart Materials and Structures*, **30**: 085005, 2021. DOI: https://doi.org/10.1088/1361-665X/ac0858.

[24] Z. M. Hu and J. Li. "Interfacial bonding effect on nonlinear magnetoelectric response of multiferroic composites. ". *Mechanics of Materials*, **153**:103660, 2021. DOI: https://doi.org/10.1016/j.mechmat.2020.103660.

[25] U. B. Bala, M. C. Krantz, and M. Gerken. "Electrode position optimization in magnetoelectric sensors based on magnetostrictive-piezoelectric bilayers on cantilever substrates. ". *IEEE Transactions on Ultrasonics, Ferroelectrics, and Frequency Control*, **61**:392–398, 2014. DOI: https://doi.org/10.1109/TUFFC.2014.2924.

[26] M.A. Indianto, M. Toda, and T. Ono. "Comprehensive study of magnetostriction-based MEMS magnetic sensor of a FeGa/PZT cantilever. ". *Sensors and Actuators A: Physical*, **331**:112985, 2021. DOI: https://doi.org/10.1016/j.sna.2021.112985.

[27] A. Lasheras, P. G. Saiz, J. M. Porro, I. Quintana, C. Polak, and A. C. Lopes. "Enhanced performance of magnetoelectric laminated composites by geometry engineering for high frequency applications.". *Journal of Alloys and Compounds*, **884**:161065, 2021. DOI: https://doi.org/10.1016/j.jallcom.2021.161065.

[28] P. Hayes, M. Jovičević Klug, S. Toxværd, P. Durdaut, V. Schell, A. Teplyuk, et al. "Converse magnetoelectric composite resonator for sensing small magnetic fields. ". *Scientific Reports*, **9**:16355, 2019. DOI: https://doi.org/10.1038/s41598-019-52657-w.

[29] M. Peddigari, K. Woo, S.-D. Kim, M. S. Kwak, J. W. Jeong, J.-H. Kang, et al. "Ultra-magnetic field sensitive magnetoelectric composite with sub-pT detection limit at low frequency enabled by flash photon annealing. ". *Nano Energy*, **90**:106598, 2021. DOI: https://doi.org/10.1016/j.nanoen.2021.106598.

[30] A. R. Will-Cole, A. E. Hassanien, S. D. Calisgan, M.-G. Jeong, X. Liang, S. Kang, et al. "Tutorial: Piezoelectric and magnetoelectric N/MEMS—Materials, devices, and applications. ". *Journal of Applied Physics*, **131**:241101, 2022. DOI: https://doi.org/10.1063/5.0094364.

[31] J. Xu, C. M. Leung, X. Zhuang, J. Li, S. Bhardwaj, J. Volakis, and D. Viehland. "A low frequency mechanical transmitter based on magnetoelectric heterostructures operated at their resonance frequency. ". *Sensors*, **19**, 2019. DOI: https://doi.org/10.3390/s19040853.

[32] J. Ou-Yang, X. Liu, H. Zhou, Z. Zou, Y. Yang, J. Li, et al. "Magnetoelectric laminate composites: an overview of methods for improving the DC and low-frequency response. ". *Journal of Physics D: Applied Physics*, **51**:324005, 2018. DOI: https://doi.org/10.1088/1361-6463/aaced8.

[33] D. K. Pradhan, S. Kumari, and P. D. Rack. "Magnetoelectric composites: Applications, coupling mechanisms, and future directions. ". *Nanomaterials*, **10**, 2020. DOI: https://doi.org/10.3390/nano10102072.

[34] X. Liang, H. Chen, and N. X. Sun. "Magnetoelectric materials and devices. ". *APL Materials*, **9**:041114, 2021. DOI: https://doi.org/10.1063/5.0044532.

[35] R. Gupta and R. K. Kotnala. "A review on current status and mechanisms of room-temperature magnetoelectric coupling in multiferroics for device applications. ". *Journal of Materials Science*, **57**:12710–37, 2022. DOI: https://doi.org/10.1007/s10853-022-07377-4.

[36] Z. Chu, M. PourhosseiniAsl, and S. Dong. "Review of multi-layered magnetoelectric composite materials and devices applications. ". *Journal of Physics D: Applied Physics*, **51**:243001, 2018. DOI: https://doi.org/10.1088/1361-6463/aac29b.

[37] K.-H. Cho. "Effect of structural control on the magnetoelectric characteristics of piezoelectric–magnetostrictive laminate composite in resonance and off-resonance modes.". *Electronic Materials Letters*, **15**:555–61, 2019. DOI: https://doi.org/10.1007/s13391-019-00151-w.

[38] Y. Zong, T. Zheng, P. Martins, S. Lanceros-Mendez, Z. Yue, and M. J. Higgins. "Cellulose-based magnetoelectric composites. ". *Nature Communications*, **8**: 38, 2017. DOI: https://doi.org/10.1038/s41467-017-00034-4.

[39] S. V. Chong and G. V. M. Williams. "Magnetoelectric effect in magnetostrictive-piezoelectric composites containing magnetite nanoparticles. ". *Sensors and Actuators A: Physical*, **288**:101–6, 2019. DOI: https://doi.org/10.1016/j.sna.2019.02.003.

[40] F. Narita and M. Fox. "A review on piezoelectric, magnetostrictive, and magnetoelectric materials and device technologies for energy harvesting applications. ". *Advanced Engineering Materials*, **20**:1700743, 2018. DOI: https://doi.org/10.1002/adem.201700743.

[41] A. Piorra, R. Jahns, I. Teliban, J. L. Gugat, M. Gerken, R. Knöchel, and E. Quandt. "Magnetoelectric thin film composites with interdigital electrodes. ". *Applied Physics Letters*, **103**:032902, 2013. DOI: https://doi.org/10.1063/1.4812706.

[42] Y. Shi, N. Li, Y. Wang, and J. Ye. "An analytical model for nonlinear magnetoelectric effect in laminated composites.". *Composite Structures*, **263**:113652, 2021. DOI: https://doi.org/10.1016/j.compstruct.2021.113652.

[43] C. Lu, H. Zhou, L. Li, A. Yang, C. Xu, Z. Ou, J. Wang, X. Wang, and M. Xin. "Split-core magnetoelectric current sensor and wireless current measurement application.". *Measurement*, **188**:110527, 2022. DOI: https://doi.org/10.1016/j.measurement.2021.110527.

[44] R. Jahns, H. Greve, E. Woltermann, E. Quandt, and R. H. Knochel. "Noise performance of magnetometers with resonant thin-film magnetoelectric sensors.". *IEEE Transactions on Instrumentation and Measurement*, **60**:2995–3001, 2011. DOI: https://doi.org/10.1109/TIM.2011.2122410.

[45] Z. Chu, Z. Jiang, Z. Mao, Y. Shen, J. Gao, and S. Dong. "Low-power eddy current detection with 1-1 type magnetoelectric sensor for pipeline cracks monitoring.". *Sensors and Actuators A: Physical*, **318**:112496, 2021. DOI: https://doi.org/10.1016/j.sna.2020.112496.

[46] Y. Qiu, L. Shi, L. Chen, Y. Yu, G. Yu, M. Zhu, and H. Zhou. "A wide-band magnetoelectric sensor based on a negative-feedback compensated readout circuit. ". *Sensors*, **24**:423, 2024. DOI: https://doi.org/10.3390/s24020423.

[47] J. Wu, Y. Du, Y. Xu, J. Qiao, Y. Qu, Z. Wang, S. Dong, Z. Hu, and M. Liu. "Self-biased magnetoelectric sensor operating in d 36 face-shear mode.". *IEEE Sensors Journal*, **23**:19, 2023. DOI: https://doi.org/10.1109/JSEN.2023.3306350.

[48] F. Li, X. Zhang, T. Wu, J. Li, X. Gao, and J. Zhu. "Enhancement of magnetoelectric coupling and anisotropy by Galfenol/PZT/Galfenol magnetoelectric sandwich device. ". *Sensors and Actuators A: Physical*, **349**:114020, 2023. DOI: https://doi.org/10.1016/j.sna.2022.114020.